Stability analysis, φ^6 model expansion method, and diverse chaos-detecting tools for the DSKP model

Mohammad Safi Ullah[1,2,*], M. Zulfikar Ali[2], Harun-Or Roshid[3,4]

[1]Department of Mathematics, Comilla University, Cumilla-3506, Bangladesh
Email: safi.ru1985@gmail.com (M.S. Ullah)
[2]Department of Mathematics, University of Rajshahi, Rajshahi-6205, Bangladesh
Email: alimath1964@gmail.com (M.Z. Ali)
[3]Department of Mathematics, Pabna University of Science and Technology, Pabna-6600, Bangladesh
Email: harunorroshidmd@gmail.com (H.O. Roshid)
[4]Department of Mathematics, Sunamgonj Science and Technology University, Sunamganj-3000, Bangladesh
[*]Corresponding Author: safi.ru1985@gmail.com (M.S. Ullah)

Abstract

This paper talks about the φ^6 -model expansion method for the Davey–Stewartson–Kadomtsev–Petviashvili (DSKP) model in (4+1) dimensions. This is useful for studying shallow-water waves, coastal engineering, fluid mechanics, and plasma physics. We use a variable relation to transform the model's partial differential form into an ordinary one. Computational software then examines the resultant model using the previously outlined methods. Combining solutions for Jacobi elliptic, hyperbolic, and trigonometric forms yields novel dynamical optical solitons. We also employ a planar dynamical process to examine the governing model qualitatively. We also investigate stability analysis, bifurcation, and chaotic behavior with diverse chaos-identification tools. The study's findings allow us to conclude that the approach is favorable, helpful, soothing, and suitable for handling a variety of nonlinear models.

Keywords: Return map; recurrence plot; equilibrium points; Lyapunov exponent; strange attractor.

1 Introduction

Nonlinear evolution equations may result from many natural occurrences in daily life. Due to dispersive and nonlinear interactions, soliton is a well-known area of nonlinear physics [1-5]. Nonlinear research uses different models like Jimbo-Miwa [6], Biswas-Arshed [7], Hirota [8], Hirota-Maccari [9], WBBM [10], and some additional nonlinear problems. The φ^6-model expansion method [11], the amended extended tanh-function algorithm [12], the F-expansion scheme [13], the modified Sardar sub-equation approach [14], and several additional new ideas have been proposed by prominent academics to characterize the features of nonlinear systems that arise in mathematical physics. Compared to the mentioned procedures, the φ^6-model expansion approach is more often used. Zhou and his colleagues discovered it for the first time in 2013 [15] and found that it had many nonlinear problems.

Rehman and others obtained precise solitary wave findings for the WBBM equation by using the method described in 2021 [16]. In 2020, Sajid and Akram investigated the Biswas-Arshed equation using this method and obtained some exact solutions [17]. In 2023, Tipu and colleagues used the chosen technique to get periodic, singular, bright, and joint singular soliton results of the Shynaray-IIA system [18]. Ullah et al. employed the stated technique to examine the soliton results of the Fokas–Lenells equation in 2023 [19].

Motivated by the above works and their intriguing features, we use the φ^6-model expansion method to find soliton solutions to the DSKP equation Eq.(2.1). Additionally, we include the planar dynamic assessment, which expands our understanding of stability, bifurcation, chaos, and other issues that previous studies have not fully explored. The φ^6-model expansion and planar dynamic processes can be used to study solitons and the dynamical parts of the governing equation for the first time in this report.

The design of the organization of this research is as follows. Section two presents the description of the φ^6-model expansion scheme. Application of the adopted scheme to the DSKP model is described in Section 3. A diagrammatic description of the answers achieved is provided in Section 4. Section 5 contains the stability study for equilibrium locations. Section 6 describes chaotic analysis using several approaches to detect chaos. Section 7 explains the novelty of these discoveries. Section 8 provides a brief description of the results.

2 Description of the φ^6-model expansion scheme

The steps that follow are the essential phases of the presented φ^6-model expansion approach [11-15]:

Step 1: Take into account the nonlinear evolution problem for $M = M(x, \mathrm{y}, \mathrm{z}, t, w)$ that follows.

$$\Xi\left(M, M_x, M_y, M_z, M_w, M_t, M_{xx}, M_{xt}, M_{xy}, \ldots\ldots\right) = 0, \tag{2.1}$$

where Ξ is a polynomial of $M(x, \mathrm{y}, \mathrm{z}, t, w)$, that contains highest-order partial derivatives with nonlinear terms.

Step 2: We offer a traveling wave transformation as

$$M(x, \mathrm{y}, \mathrm{z}, t, w) = Q(\varsigma), \tag{2.2}$$

for the soliton's magnitude component Q and $\varsigma = ax + by + cz + dw - et$ has a soliton speed of e. Then Eq.(2.1) will be converted to the next ordinary differential form

$$\Omega(M, M', MM', M'', \ldots\ldots) = 0, \tag{2.3}$$

where the prime "$'$" indicates the derivative of M related to ς.

Step 3: We use the following trial solution for Eq. (2.3).

$$Q(\varsigma) = \sum_{i=0}^{2K} p_i u(\varsigma)^i, \tag{2.4}$$

where p_i $(i = 0, 1, 2, \ldots, 2K)$ are arbitrary amounts and $u(\varsigma)$ fulfilled the following auxiliary differential forms

$$\begin{cases} u'^2(\varsigma) = q_0 + q_2 u^2(\varsigma) + q_4 u^4(\varsigma) + q_6 u^6(\varsigma) \\ u''(\varsigma) = q_2 u(\varsigma) + 2q_4 u^3(\varsigma) + 3q_6 u^5(\varsigma) \end{cases} \tag{2.5}$$

with real constants q_0, q_2, q_4, and q_6.

Step 4: It has become widely reputed that the following relationship is satisfied by Eq.(2.5)

$$u(\varsigma) = \frac{v(\varsigma)}{\sqrt{f v^2(\varsigma)+g}}, \tag{2.6}$$

in which $0 < f v^2(\varsigma) + g$ and the Jacobi elliptic formula has been satisfied by $v(\varsigma)$, where

$$v'^2(\varsigma) = s_0 + s_2 v^2(\varsigma) + s_4 v^4(\varsigma), \tag{2.7}$$

for unknown amounts $s_i (i = 0,2,4)$, when f and g are given by

$$f = \frac{q_4(s_2-q_2)}{(s_2-q_2)^2+3s_0s_4-2s_2(s_2-q_2)}, \tag{2.8}$$

$$g = \frac{3s_0q_4}{(s_2-q_2)^2+3s_0s_4-2s_2(s_2-q_2)} \tag{2.9}$$

for the constraint relation

$$q_4^2(s_2-q_2)(9s_0s_4-(s_2-q_2)(2s_2+q_2)) + 3q_6(-s_2^2+q_2^2+3s_0s_4)^2 = 0. \tag{2.10}$$

Step 5: It is well known that Eq.(2.7) gives the following Jacobi elliptic solutions that include $0 < \varrho < 1$. Replacing Eq.(2.7) along with Eq.(2.6) into Eq.(2.4) one reaches the exact results of Eq.(2.1).

Function	$\varrho \to 1$	$\varrho \to 0$	Function	$\varrho \to 1$	$\varrho \to 0$
$dn(\varsigma, \varrho)$	$sech(\varsigma)$	1	$sd(\varsigma, \varrho)$	$sinh(\varsigma)$	$sin(\varsigma)$
$cn(\varsigma, \varrho)$	$sech(\varsigma)$	$cos(\varsigma)$	$sc(\varsigma, \varrho)$	$sinh(\varsigma)$	$tan(\varsigma)$
$dc(\varsigma, \varrho)$	1	$sec(\varsigma)$	$nd(\varsigma, \varrho)$	$cosh(\varsigma)$	1
$cs(\varsigma, \varrho)$	$csch(\varsigma)$	$cot(\varsigma)$	$cd(\varsigma, \varrho)$	1	$cos(\varsigma)$
$sn(\varsigma, \varrho)$	$tanh(\varsigma)$	$sin(\varsigma)$	$ds(\varsigma, \varrho)$	$csch(\varsigma)$	$csc(\varsigma)$
$ns(\varsigma, \varrho)$	$coth(\varsigma)$	$csc(\varsigma)$	$nc(\varsigma, \varrho)$	$cosh(\varsigma)$	$sec(\varsigma)$

3 Applications of the adopted scheme to the DSKP model

The present study considers the DSKP model, as illustrated below [20, 21]:

$$4M_{xt} - M_{xxxy} + M_{xyyy} + 12M_xM_y + 12MM_{xy} - 6M_{zw} = 0. \tag{3.1}$$

Here, $M(\mathrm{t}, x, y, z, w)$ represents the soliton magnitude, which includes the time component t and the space variables x, y, z, and w. Fokas, a well-known Greek scientist, first created this model by expanding the solvable Davey-Stewartson and Kadomtsev-Petviashvili nonlinear equations [22]. Ref. [23] shows Eq.(3.1) represents both elastic and non-elastic internal relationships between wave shapes. We can use this more complex framework [24] to model several nonlinear problems in shallow water waves and plasma physics.

The conversion relationship is taken into consideration below to get the soliton results for Eq.(3.1):

$$M(x, \mathrm{y}, \mathrm{z}, t, w) = Q(\varsigma), \tag{3.2}$$

for the soliton's magnitude component Q and $\varsigma = ax + by + cz + dw - et$ has a soliton speed of e. According to Eq.(3.1) and Eq.(3.2), we obtain

$$(ab^3 - a^3\mathrm{b})\mathrm{Q}^{iv} + 12abQQ'' + 12abQ'^2 - (4ae - 6dc)Q'' = 0. \tag{3.3}$$

Following two rounds of integration regarding ς in Eq.(3.3), one arives at

$$(ab^3 - a^3b)Q'' + 6abQ^2 - (4ae + 6dc)Q = 0. \tag{3.4}$$

By comparing Q'' with Q^2 produces $K = 2$, and Eq.(2.4) can be stated as follows:

$$Q(\varsigma) = p_0 + p_1u(\varsigma) + p_2u(\varsigma)^2 + p_3u(\varsigma)^3 + p_4u(\varsigma)^4, \tag{3.5}$$

when p_0, p_1, p_2, p_3, and p_4 all are real numbers. Combining Eqs.(3.4), (3.5), and (2.5) with some modifications, one reaches the next outcomes

$$\begin{cases} e = \frac{2ab^3q_2 + 6abp_0 - 2a^3bq_2 - 3cd}{2\mathrm{a}}, p_2 = (a^2 - b^2)q_4, q_0 = \frac{p_0(2a^2q_2 - 2b^2q_2 - 3p_0)}{q_4(a^4 - 2a^2b^2 + b^4)}, \\ p_1 = 0, p_3 = 0, p_4 = 0, p_0 = p_0, q_2 = q_2, q_4 = q_4, q_6 = 0, \end{cases} \tag{3.6}$$

$$
\begin{cases}
e = -\frac{1}{4q_6 a(a^2{q_4}^2 - b^2{q_4}^2 - 8p_0 q_6)}(a^5 b{q_4}^4 - 2a^3b^3{q_4}^4 - 12a^3bp_0{q_4}^2q_6 + 12ab^3p_0{q_4}^2q_6 \\
+ab^5{q_4}^4 + 6a^2cd{q_4}^2q_6 - 6b^2cd{q_4}^2q_6 + 48abp_0{}^2{q_6}^2 - 48cdp_0{q_6}^2), p_0 = p_0, p_1 = 0, \\
p_2 = 2a^2q_4 - 2b^2q_4, p_3 = 0, p_4 = 4a^2q_6 - 4b^2q_6, q_0 = \frac{p_0q_4(a^2{q_4}^2 - b^2{q_4}^2 - 6p_0q_6)}{4q_6(a^2-b^2)(a^2{q_4}^2 - b^2{q_4}^2 - 8p_0q_6)}, \\
\quad q_2 = \frac{a^4{q_4}^4 - 2a^2b^2{q_4}^4 + b^4{q_4}^4 - 6a^2p_0{q_4}^2q_6 + 6b^2p_0{q_4}^2q_6 - 12{p_0}^2{q_6}^2)}{4q_6(a^2-b^2)(a^2{q_4}^2 - b^2{q_4}^2 - 8p_0q_6)}, q_4 = q_4, q_6 = q_6.
\end{cases} \tag{3.7}
$$

Using Eqs. (3.5), (3.6), and (2.6), along with the table mentioned above, yields the subsequent soliton results of Eq.(3.1).

1. If $s_0 = 1$, $s_2 = -(1+\varrho^2)$, $s_4 = \varrho^2$, $0 < \varrho < 1$, one gets $v(\varsigma)$ equal $sn(\varsigma,\varrho)$ or $cd(\varsigma,\varrho)$ and then

$$M_{1,1}(x, y, z, t, w) = \left(\frac{(sn(\varsigma,\varrho))^2}{f(sn(\varsigma,\varrho))^2 + g}\right)p_2$$

or

$$M_{1,2}(x, y, z, t, w) = \left(\frac{(cd(\varsigma,\varrho))^2}{f(cd(\varsigma,\varrho))^2 + g}\right)p_2$$

including $f = \frac{(1+\varrho^2+q_2)q_4}{1-\varrho^2+\varrho^4-q_2^2}$, and $g = \frac{-3q_4}{1-\varrho^2+\varrho^4-q_2^2}$ with the constraint relation $q_4^2(q_2 + 1 + \varrho^2)(-q_2 + 2\varrho^2 - 1)(q_2 + \varrho^2 - 2) = 0$.

For $\varrho \to 1$, one reaches the next periodic wave outcome

$$M_{1,3}(x, y, z, t, w) = \left(\frac{(tanh(\varsigma))^2}{\frac{q_4(q_2+2)(tanh(\varsigma))^2 - 3q_4}{1-q_2^2}}\right)p_2$$

such that $q_4^2(-1+q_2)^2(2+q_2) = 0$.

For $\varrho \to 0$, we obtain the underneath singular periodic wave solution

$$M_{1,4}(x, y, z, t, w) = \left(\frac{(sin(\varsigma))^2}{\frac{q_4(1+q_2)(sin(\varsigma))^2 - 3q_4}{q_2^2-1}}\right)p_2$$

or

$$M_{1,5}(x, y, z, t, w) = \left(\frac{(cos(\varsigma))^2}{\frac{q_4(1+q_2)(cos(\varsigma))^2 - 3q_4)}{1-q_2^2}}\right)p_2$$

where $q_4^2(q_2-2)(1+q_2)^2=0$.

2. If $s_0=1-\varrho^2,\ s_2=2\varrho^2-1,\ s_4=-\varrho^2,\ 0<\varrho<1$, then $v(\varsigma)=cn(\varsigma,\varrho)$ and we have

$$M_{2,1}(x,\mathrm{y},\mathrm{z},t,w)=\left(\frac{(cn(\varsigma,\varrho))^2}{f(cn(\varsigma,\varrho))^2+g}\right)p_2$$

such that $f=\frac{q_4(1-2\varrho^2+q_2)}{1-\varrho^2+\varrho^4-q_2^2}$, and $g=\frac{3q_4(\varrho^2-1)}{1-\varrho^2+\varrho^4-q_2^2}$ with the constraint relation $q_4^2(-1-q_2+2\varrho^2)(\varrho^2+q_2+1)(-2+\varrho^2+q_2)=0$.

For $\varrho\rightarrow 0$, we get the underneath singular periodic wave solution

$$M_{2,2}(x,\mathrm{y},\mathrm{z},t,w)=\left(\frac{(cos(\varsigma))^2}{\frac{q_4(1+q_2)(cos(\varsigma))^2-3q_4}{1-q_2^2}}\right)p_2$$

where $q_4^2(1+q_2)^2(-2+q_2)=0$.

3. If $s_0=\varrho^2-1,\ s_2=-\varrho^2+2,\ s_4=-1,\ 0<\varrho<1$, then $v(\varsigma)=dn(\varsigma,\varrho)$ which reads

$$M_3(x,\mathrm{y},\mathrm{z},t,w)=\left(\frac{(dn(\varsigma,\varrho))^2}{f(dn(\varsigma,\varrho))^2+g}\right)p_2$$

including $f=\frac{q_4(-2+\varrho^2+q_2)}{1-\varrho^2+\varrho^4-q_2^2}$, and $g=\frac{-3q_4(\varrho^2-1)}{1-\varrho^2+\varrho^4-q_2^2}$ with the constraint relation $q_4^2(q_2+\varrho^2+1)(-1-q_2+2\varrho^2)(\varrho^2+q_2-2)=0$.

4. If $s_0=\varrho^2,\ s_2=-(\varrho^2+1),\ s_4=1,\ 0<\varrho<1$, one reaches $v(\varsigma)$ equal $ns(\varsigma,\varrho)$ or $dc(\varsigma,\varrho)$ and then

$$M_{4,1}(x,\mathrm{y},\mathrm{z},t,w)=\left(\frac{(ns(\varsigma,\varrho))^2}{f(ns(\varsigma,\varrho))^2+g}\right)p_2$$

or

$$M_{4,2}(x,\mathrm{y},\mathrm{z},t,w)=\left(\frac{(dc(\varsigma,\varrho))^2}{f(dc(\varsigma,\varrho))^2+g}\right)p_2$$

such that $f=\frac{q_4(q_2+\varrho^2+1)}{1-\varrho^2+\varrho^4-q_2^2}$, and $g=\frac{-3q_4\varrho^2}{1-\varrho^2+\varrho^4-q_2^2}$ with the constraint relation $q_4^2(-1+2\varrho^2-q_2)(\varrho^2+q_2-2)(\varrho^2+q_2+1)=0$.

For $\varrho\rightarrow 1$, one can obtain the underneath singular soliton result

$$M_{4,3}(x,\mathrm{y},\mathrm{z},t,w)=\left(\frac{(coth(\varsigma))^2}{\frac{q_4(2+q_2)(co\quad(\varsigma))^2-3q_4}{1-q_2^2}}\right)p_2$$

such that $q_4^2(-1+q_2)^2(2+q_2)=0$.

5. If $s_0=-\varrho^2,\ s_2=2\varrho^2-1,\ s_4=1-\varrho^2,\ 0<\varrho<1$, then $v(\varsigma)=nc(\varsigma,\varrho)$ and we have

$$M_{5,1}(x,\mathrm{y},\mathrm{z},t,w)=\left(\frac{(nc(\varsigma,\varrho))^2}{f(nc(\varsigma,\varrho))^2+g}\right)p_2$$

such that $f=\frac{-(-1+2\varrho^2-q_2)q_4}{1-\varrho^2+\varrho^4-q_2^2}$, and $g=\frac{3q_4\varrho^2}{1-\varrho^2+\varrho^4-q_2^2}$ with the constraint relation $q_4^2(-1+2\varrho^2-q_2)(\varrho^2+q_2-2)(\varrho^2+q_2+1)=0$.

For $\varrho\rightarrow 1$, one reaches the next singular soliton solution

$$M_{5,2}(x,\mathrm{y},\mathrm{z},t,w)=\left(\frac{(cosh(\varsigma))^2}{\frac{-q_4(1-q_2)(cosh(\varsigma))^2+3q_4}{1-q_2^2}}\right)p_2$$

such that $q_4^2(-1+q_2)^2(2+q_2)=0$.

6. If $s_0=-1,\ s_2=2-\varrho^2,\ s_4=\varrho^2-1,\ 0<\varrho<1$, then $v(\varsigma)=nd(\varsigma,\varrho)$ and we have

$$M_{6,1}(x,\mathrm{y},\mathrm{z},t,w)=\left(\frac{(nd(\varsigma,\varrho))^2}{f(nd(\varsigma,\varrho))^2+g}\right)p_2$$

such that $f=\frac{(q_2+\varrho^2-2)q_4}{1-\varrho^2+\varrho^4-q_2^2}$, and $g=\frac{3q_4}{1-\varrho^2+\varrho^4-q_2^2}$ with the constraint relation $q_4^2(-1+2\varrho^2-q_2)(\varrho^2+q_2-2)(\varrho^2+q_2+1)=0$.

If $\varrho\rightarrow 1$, we acquire the following singular-wave solution

$$M_{6,2}(x,\mathrm{y},\mathrm{z},t,w)=\left(\frac{(cosh(\varsigma))^2}{\frac{q_4(-1+q_2)(cosh(\varsigma))^2+3q_4}{1-q_2^2}}\right)p_2$$

while $q_4^2(-1+q_2)^2(2+q_2)=0$.

7. If $s_0=1,\ s_2=2-\varrho^2,\ s_4=1-\varrho^2,\ 0<\varrho<1$, then $v(\varsigma)=sc(\varsigma,\varrho)$ and we have

$$M_{7,1}(x,\mathrm{y},\mathrm{z},t,w)=\left(\frac{(sc(\varsigma,\varrho))^2}{f(sc(\varsigma,\varrho))^2+g}\right)p_2$$

such that $f=\frac{q_4(q_2+\varrho^2-2)}{1-\varrho^2+\varrho^4-q_2^2}$, and $g=\frac{-3q_4}{1-\varrho^2+\varrho^4-q_2^2}$ with the constraint relation $q_4^2(-1+2\varrho^2-q_2)(\varrho^2+q_2-2)(\varrho^2+q_2+1)=0$.

If $\varrho\to 1$, we get a soliton outcome

$$M_{7,2}(x,\mathrm{y},\mathrm{z},t,w)=\left(\frac{(sinh(\varsigma))^2}{\frac{q_4(-1+q_2)(sinh(\varsigma))^2-3q_4}{1-q_2^2}}\right)p_2$$

while $q_4^2(-1+q_2)^2(2+q_2)=0$.

For $\varrho\to 0$, one gains the underneath periodic singular periodic wave solutions

$$M_{7,3}(x,\mathrm{y},\mathrm{z},t,w)=\left(\frac{(tan(\varsigma))^2}{\frac{q_4(-2+q_2)(tan(\varsigma))^2-3q_4}{1-q_2^2}}\right)p_2$$

whereas $q_4^2(1+q_2)^2(-2+q_2)=0$.

8. If $s_0=1,\ s_2=2\varrho^2-1,\ s_4=-\varrho^2(1-\varrho^2),\ 0<\varrho<1$, then $v(\varsigma)=sd(\varsigma,\varrho)$ and we have

$$M_{8,1}(x,\mathrm{y},\mathrm{z},t,w)=\left(\frac{(sd(\varsigma,\varrho))^2}{f(sd(\varsigma,\varrho))^2+g}\right)p_2$$

such that $f=\frac{-(2\varrho^2-q_2-1)q_4}{1-\varrho^2+\varrho^4-q_2^2}$, and $g=\frac{-3q_4}{1-\varrho^2+\varrho^4-q_2^2}$ with the constraint relation $q_4^2(-1+2\varrho^2-q_2)(\varrho^2+q_2-2)(\varrho^2+q_2+1)=0$.

For $\varrho\to 1$, one reaches the next soliton result

$$M_{8,2}(x,\mathrm{y},\mathrm{z},t,w)=\left(\frac{(sin\ \ (\varsigma))^2}{\frac{-q_4(1-q_2)(sin\ \ (\varsigma))^2-3q_4}{1-q_2^2}}\right)p_2$$

whereas $q_4^2(-1+q_2)^2(2+q_2)=0$.

If $\varrho\to 0$, we obtain the next singular periodic waveform result

$$M_{8,3}(x,\mathrm{y},\mathrm{z},t,w)=\left(\frac{(sinh(\varsigma))^2}{\frac{q_4(1+q_2)(sinh(\varsigma))^2-3q_4}{1-q_2^2}}\right)p_2$$

where $q_4^2(1+q_2)^2(-2+q_2)=0$.

9. If $s_0=1-\varrho^2,\ s_2=2-\varrho^2,\ s_4=1,\ 0<\varrho<1$, then $v(\varsigma)=cs(\varsigma,\varrho)$ and we have

$$M_{9,1}(x,\mathrm{y},\mathrm{z},t,w)=\left(\frac{(cs(\varsigma,\varrho))^2}{f(cs(\varsigma,\varrho))^2+g}\right)p_2$$

such that $f=\frac{(\varrho^2+q_2-2)q_4}{1-\varrho^2+\varrho^4-q_2^2}$, and $g=\frac{3q_4(-1+\varrho^2)}{1-\varrho^2+\varrho^4-q_2^2}$ with the constraint relation $q_4^2(-1+2\varrho^2-q_2)(\varrho^2+q_2-2)(\varrho^2+q_2+1)=0$.

For $\varrho\to 0$, we attain the underneath singular periodic wave solution

$$M_{9,2}(x,\mathrm{y},\mathrm{z},t,w)=\left(\frac{(cot(\varsigma))^2}{\frac{q_4(-2+q_2)(cot(\varsigma))^2-3q_4}{1-q_2^2}}\right)p_2$$

with $q_4^2(1+q_2)^2(-2+q_2)=0$.

10. If $s_0=-\varrho^2(1-\varrho^2),\ s_2=2\varrho^2-1,\ s_4=1,\ 0<\varrho<1$, then $v(\varsigma)=ds(\varsigma,\varrho)$ and we have

$$M_{10}(x,\mathrm{y},\mathrm{z},t,w)=\left(\frac{(ds(\varsigma,\varrho))^2}{f(ds(\varsigma,\varrho))^2+g}\right)p_2$$

such that $f=\frac{-(2\varrho^2-q_2-1)q_4}{1-\varrho^2+\varrho^4-q_2^2}$, and $g=\frac{-3q_4\varrho^2(-1+\varrho^2)}{1-\varrho^2+\varrho^4-q_2^2}$ with the constraint condition $q_4^2(-1+2\varrho^2-q_2)(\varrho^2+q_2-2)(q_2+\varrho^2+1)=0$.

11. If $s_0=\frac{-\varrho^2+1}{4}$, $s_2=\frac{\varrho^2+1}{2}$, $s_4=\frac{-\varrho^2+1}{4}$, $0<\varrho<1$, one reaches $v(\varsigma)$ equal

$nc(\varsigma,\varrho) \pm sc(\varsigma,\varrho)$ or $\frac{cn(\varsigma,\varrho)}{1\pm sn(\varsigma,\varrho)}$ and then

$$M_{11,1}(x,\mathrm{y},\mathrm{z},t,w) = \left(\frac{(nc(\varsigma,\varrho)\pm sc(\varsigma,\varrho))^2}{f(nc(\varsigma,\varrho)\pm sc(\varsigma,\varrho))^2+g}\right)p_2$$

or

$$M_{11,2}(x,\mathrm{y},\mathrm{z},t,w) = \left(\frac{\left(\frac{cn(\varsigma,\varrho)}{1\pm sn(\varsigma,\varrho)}\right)^2}{f\left(\frac{cn(\varsigma,\varrho)}{1\pm sn(\varsigma,\varrho)}\right)^2+g}\right)p_2$$

such that $f = \frac{-8q_4(1+\varrho^2-2q_2)}{1+14\varrho^2+\varrho^4-16q_2^2}$, and $g = \frac{12q_4(-1+\varrho^2)}{1+14\varrho^2+\varrho^4-16q_2^2}$ with the constraint condition $\frac{1}{32}q_4^2(1+\varrho^2-2q_2)(4q_2+\varrho^2-6\varrho+1)(1+\varrho^2+6\varrho+4q_2)=0$.

For $\varrho \to 0$, we obtain the underneath singular periodic wave solution

$$M_{11,3}(x,\mathrm{y},\mathrm{z},t,w) = \left(\frac{(sec(\varsigma)\pm tan(\varsigma))^2}{\frac{-8q_4(1-2q_2)(sec(\varsigma)\pm tan(\varsigma))^2-12q_4}{1-16q_2^2}}\right)p_2$$

or

$$M_{11,4}(x,\mathrm{y},\mathrm{z},t,w) = \left(\frac{\left(\frac{cos(\varsigma)}{1\pm sin(\varsigma)}\right)^2}{\frac{-8q_4(1-2q_2)\left(\frac{cos(\varsigma)}{1\pm sin(\varsigma)}\right)^2-12q_4}{1-16q_2^2}}\right)p_2$$

such that $\frac{1}{32}q_4^2(1-2q_2)(4q_2+1)^2=0$.

12. If $s_0 = \frac{-(1-\varrho^2)^2}{4}$, $s_2 = \frac{1+\varrho^2}{2}$, $s_4 = -\frac{1}{4}$, $0<\varrho<1$, then $v(\varsigma) = \varrho cn(\varsigma,\varrho) \pm dn(\varsigma,\varrho)$ and degenerated to

$$M_{12}(x,\mathrm{y},\mathrm{z},t,w) = \left(\frac{(\varrho cn(\varsigma,\varrho)\pm dn(\varsigma,\varrho))^2}{f(\varrho cn(\varsigma,\varrho)\pm dn(\varsigma,\varrho))^2+g}\right)p_2$$

such that $f = \frac{-8q_4(1+\varrho^2-2q_2)}{1+14\varrho^2+\varrho^4-16q_2^2}$, and $g = \frac{12q_4(-1+\varrho^2)^2}{1+14\varrho^2+\varrho^4-16q_2^2}$ with the constraint condition $\frac{1}{32}q_4^2(1+\varrho^2-2q_2)(4q_2+\varrho^2-6\varrho+1)(1+\varrho^2+6\varrho+4q_2)=0$.

13. If $s_0 = \frac{1}{4}$, $s_2 = \frac{1-2\varrho^2}{2}$, $s_4 = \frac{1}{4}$, $0<\varrho<1$, then $v(\varsigma) = \frac{sn(\varsigma,\varrho)}{1\pm cn(\varsigma,\varrho)}$ and we have

$$M_{13,1}(x, \mathrm{y}, \mathrm{z}, t, w) = \left(\frac{\left(\frac{sn(\varsigma,\varrho)}{1\pm cn(\varsigma,\varrho)}\right)^2}{f\left(\frac{sn(\varsigma,\varrho)}{1\pm cn(\varsigma,\varrho)}\right)^2 + g} \right) p_2$$

such that $f = \frac{8q_4(-1+2\varrho^2+2q_2)}{1-16\varrho^2+16\ {}^{4}-16q_2^2}$, and $g = -\frac{12q_4}{1-16\varrho^2+16\varrho^4-16q_2^2}$ with the constraint condition

$\frac{1}{32}q_4^2(-1+2\varrho^2+2q_2)(16q_2\varrho^2 - 16{q_2}^2 - 8q_2 + 32\varrho^4 - 32\varrho^2 - 1) = 0.$

For $\varrho \to 1$, one reaches the following soliton and singular soliton outcomes

$$M_{13,2}(x, \mathrm{y}, \mathrm{z}, t, w) = \left(\frac{\left(\frac{tanh(\varsigma)}{1\pm sech(\varsigma)}\right)^2}{\frac{8q_4(1+2q_2)\left(\frac{tanh(\varsigma)}{1\pm sech(\varsigma)}\right)^2 - 12q_4}{1-16q_2^2}} \right) p_2$$

such that $-\frac{1}{32}q_4^2(1+2q_2)(4q_2-1)^2 = 0.$

If $\varrho \to 0$, we reach the underneath periodic singular wave outcome

$$M_{13,3}(x, \mathrm{y}, \mathrm{z}, t, w) = \left(\frac{\left(\frac{sin(\varsigma)}{1\pm cos(\varsigma)}\right)^2}{\frac{8q_4(-1+2q_2)\left(\frac{sin(\varsigma)}{1\pm cos(\varsigma)}\right)^2 - 12q_4}{1-16q_2^2}} \right) p_2$$

such that $-\frac{1}{32}q_4^2(-1+2q_2)(4q_2+1)^2 = 0.$

14. If $s_0 = \frac{1}{4}$, $s_2 = \frac{\varrho^2+1}{2}$, $s_4 = \frac{(1-\varrho^2)^2}{4}$, $0 < \varrho < 1$, one can obtain $v(\varsigma) = \frac{sn(\varsigma,\varrho)}{cn(\varsigma,\varrho)\pm dn(\varsigma,\varrho)}$ and then

$$M_{14,1}(x, \mathrm{y}, \mathrm{z}, t, w) = \left(\frac{\left(\frac{sn(\varsigma,\varrho)}{cn(\varsigma,\varrho)\pm dn(\varsigma,\varrho)}\right)^2}{f\left(\frac{sn(\varsigma,\varrho)}{cn(\varsigma,\varrho)\pm dn(\varsigma,\varrho)}\right)^2 + g} \right) p_2$$

such that $f = -\frac{8q_4(1+\varrho^2-2q_2)}{1+14\varrho^2+\varrho^4-16q_2^2}$, and $g = -\frac{12q_4}{1+14\varrho^2+\varrho^4-16q_2^2}$ with the constraint condition

$\frac{1}{32}q_4^2(1+\varrho^2-2q_2)(4q_2+\varrho^2+6\varrho+1)(4q_2+\varrho^2-6\varrho+1) = 0.$

For $\varrho \to 1$, we obtain the next soliton result

$$M_{14,2}(x,\mathrm{y},\mathrm{z},t,w)=\left(\frac{\left(\frac{tanh(\varsigma)}{sech(\varsigma)+sech(\varsigma)}\right)^2}{\frac{-4q_4(1-q_2)\left(\frac{tanh(\varsigma)}{sech(\varsigma)+sech(\varsigma)}\right)^2-3q_4}{4(1-q_2^2)}}\right)p_2$$

such that $-q_4^2(2+q_2)(q_2-1)^2=0$.

For $\varrho\to 0$, we attain the following singular periodic wave findings

$$M_{14,3}(x,\mathrm{y},\mathrm{z},t,w)=\left(\frac{\left(\frac{sin(\varsigma)}{cos(\varsigma)\pm 1}\right)^2}{\frac{-8q_4(1-2q_2)\left(\frac{sin(\varsigma)}{cos(\varsigma)\pm 1}\right)^2-12q_4}{1-16q_2^2}}\right)p_2$$

such that $-\frac{1}{32}q_4^2(4q_2+1)^2(-1+2q_2)=0$.

Now, by using Eqs. (3.5), and (3.7) with (2.6), one reaches analogous exact results as for Eq.(3.1).

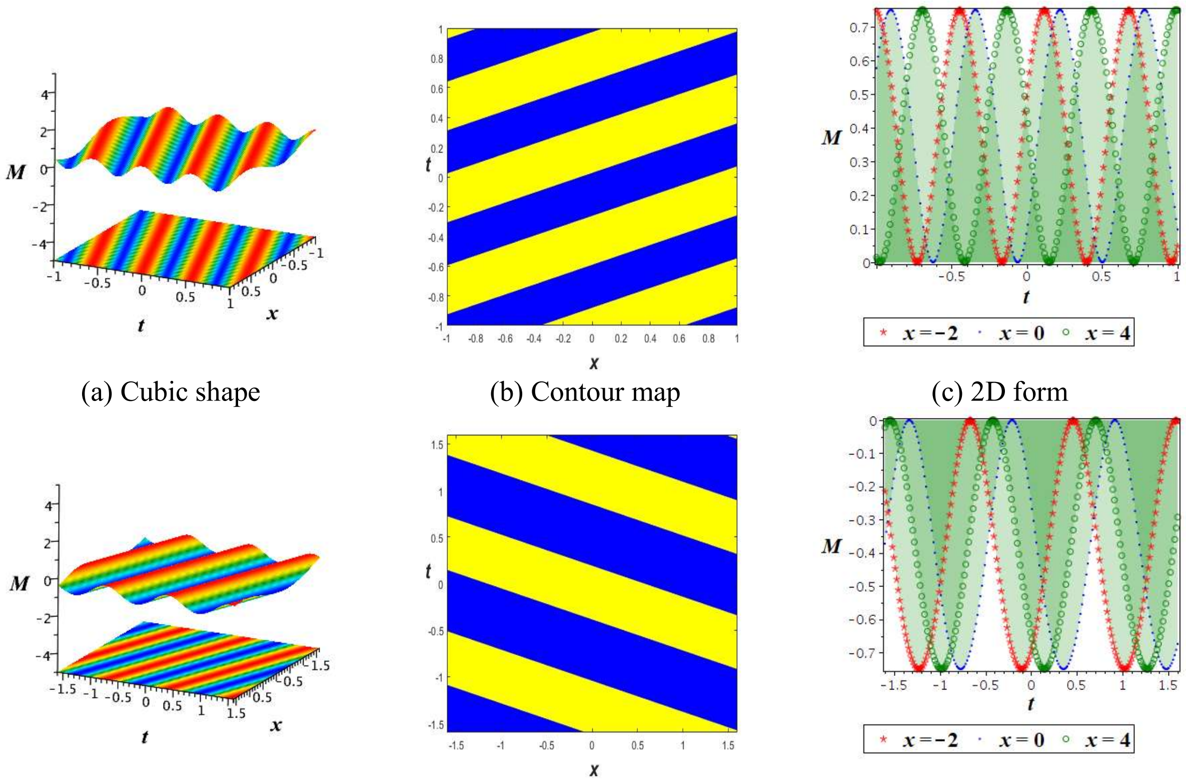

(a) Cubic shape (b) Contour map (c) 2D form

(d) Cubic shape (e) Contour map (f) 2D form

Fig-1: Graphics of W-shaped periodic wave soliton $M_{1,1}$. (a-c) denote bright shapes for $a=2$, $b=1$, while (b-d) signify dark shapes for $b=2,\ a=1$.

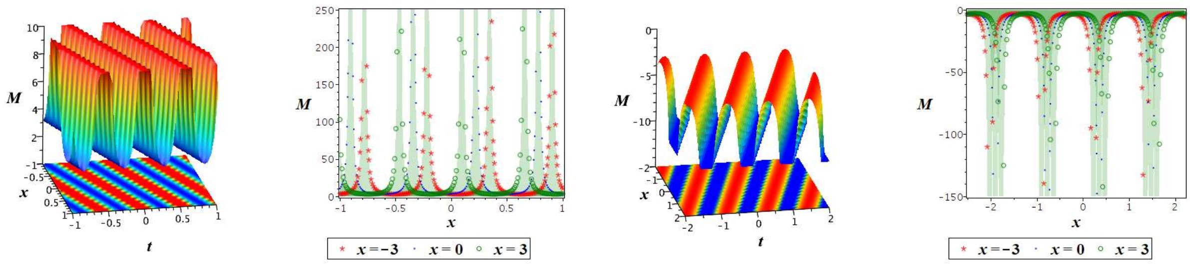

(a) (b) (c) (d)

Fig-2: Graphics of singular periodic wave outcome M_3. (a, b) denote bright shapes for $b = 1$, $a = 2$, while (c, d) signify dark shapes for $a = 1$, $b = 2$.

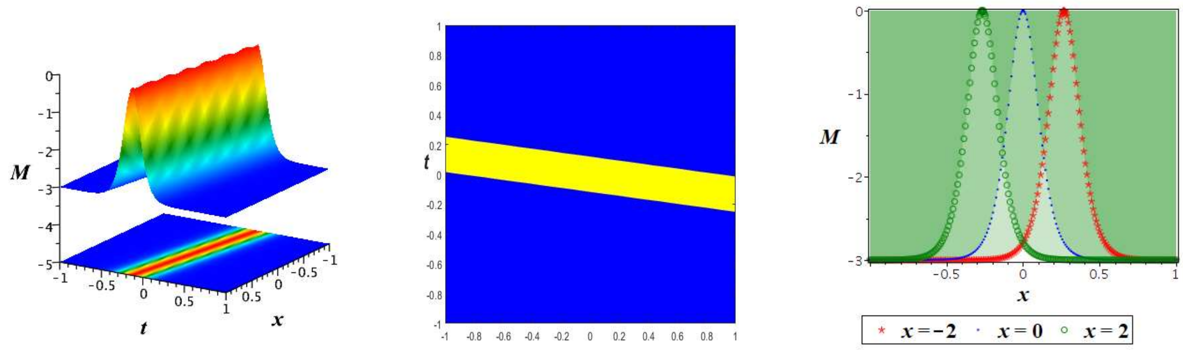

(a) Cubic form (b) Contour map (c) 2D form

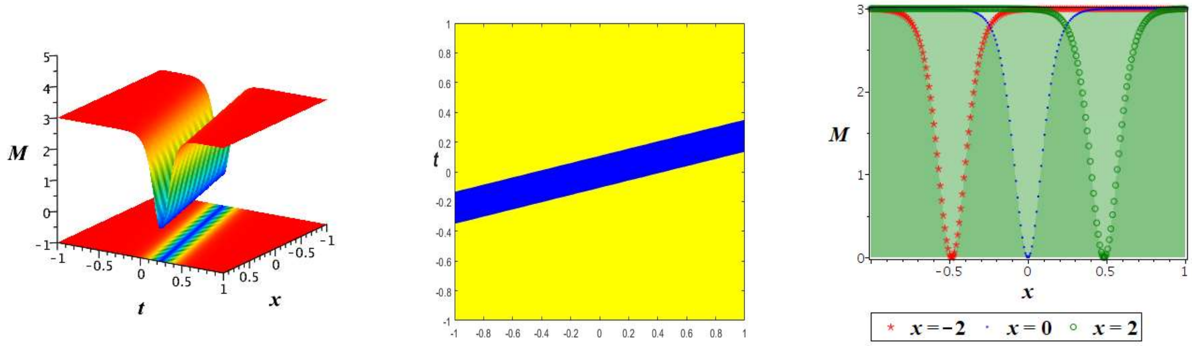

(d) Cubic form (e) Contour map (f) 2D form

Fig-3: Waveform of solution $M_{7,2}$. (a-c) bright shape for $a = 1,\ b = 2$, and (b-d) dark shape for $b = 1,\ a = 2$.

4 Graphical illustration

Solutions $M_{1,1}$, $M_{1,2}$, $M_{1,3}$ $M_{2,1}$, $M_{7,1}$, $M_{8,1}$, $M_{9,1}$ M_{12} and $M_{14,1}$ exhibit analogous waveform as reported in **Fig.1** by $M_{1,1}$ for $p_0 = q_4 = b = c = d = 1, a = 2, \varrho = 0.5, q_2 = -1.2$ at $y = z = w = 1$. We plot 3D with density, contour, and 2D graphics of this outcome displayed w-shaped periodic wave with bright soliton for $a = 2, b = 1$, dark soliton for $a = 1, b = 2$.

Solutions $M_{1,4}$, $M_{1,5}$, $M_{2,2}$, M_3, $M_{4,1}$, $M_{4,2}$, $M_{5,1}$, $M_{6,1}$, $M_{7,3}$, $M_{8,3}$, $M_{9,2}$, M_{10}, $M_{11,1}$, $M_{11,2}$, $M_{11,3}$, $M_{11,4}$, $M_{13,1}$, $M_{13,3}$, and $M_{14,3}$ demonstrate equivalent nature as discovered in **Fig.2** by M_3 for $q_4 = p_0 = c = d = 1, \varrho = 0.5, q_2 = -1.25$ at $y = z = w = 1$. We plot 3D with density, contour, and 2D graphics of M_3 displayed w-shaped periodic wave with singularity. It represents bright soliton for $a = 1,\ b = 2$, dark soliton for $a = 2,\ b = 1$. Solutions $M_{7,2}$, $M_{8,2}$, $M_{13,2}(+ve)$, and $M_{14,2}$ show the equivalent waveform as presented in **Fig.3** by $M_{7,2}$ with $d = p_0 = q_4 = b = c = \varrho = 1, a = 2, q_2 = -2$ at $w = y = z = 0.$ We plot 3D with density and 2D graphics of $S_{7,2}$ displayed soliton solution. It represent bright soliton for $a = 1,\ b = 2$ and dark soliton for $a = 2,\ b = 1.$ Solutions $M_{4,3}$, $M_{5,2}$, $M_{6,2}$, and $M_{13,2}(-ve)$ exhibit similar nature as depicted in **Fig.4** by $M_{5,2}$ for $d = q_4 = p_0 = c = \varrho = 1, q_2 = -2$ at $w = y = z = 0.$ We plot 3D with density and 2D graphics of $M_{5,2}$ displayed soliton solution with singularity. It represent bright soliton for $a = 1,\ b = 2$ and dark soliton for $a = 2,\ b = 1.$

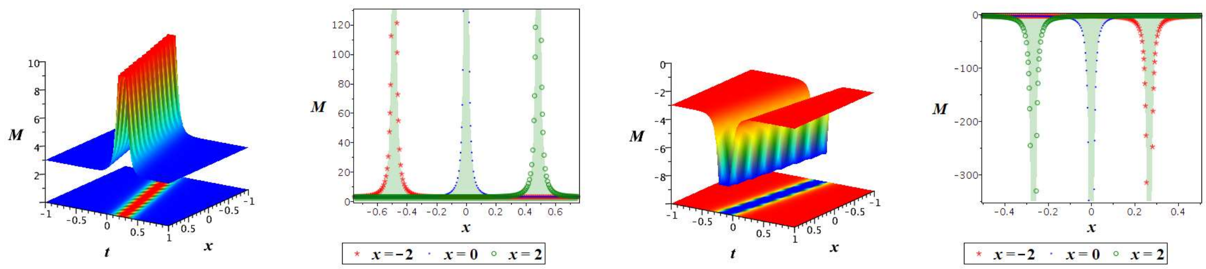

(a) (b) (c) (d)

Fig-4: Outlook of singular waveform $M_{5,2}$. (a, b) denote bright shapes for $a = 2,\ b = 1$, while (c, d) signify dark shapes for $a = 1,\ b = 2$.

5 Stability examination for the equilibrium points

The equilibrium evaluation of the governing model is discussed in this segment using a planar dynamical system [25]. The arrangement of variables in Eq.(3.4) can be expressed as the next dynamical system to facilitate this investigation.

$$\frac{\mathrm{dQ}}{\mathrm{d}\varsigma} = Y, \frac{\mathrm{d}Y}{\mathrm{d}\varsigma} = \omega_1 Q + \omega_2 Q^2. \tag{5.1}$$

where $\omega_1 = \frac{4ae+6dc}{ab^3-a^3b}$ and $\omega_2 = -\frac{6ab}{ab^3-a^3b}$. This system presents well-known phase pictures in the (Q, Y)-plane, which includes parameters a, $b, c, d,$ and e related to DSKP model soliton solutions. The formulations $Q' = \frac{\partial H}{\partial Y}$ and $Y' = -\frac{\partial H}{\partial Q}$ famous for Hamilton's canonical formula deriving either Eq (3.4) or Eq (5.1) from the subsequent Hamiltonian function.

$$H(Q, Y) = \frac{1}{2}Y^2 + \frac{2ab}{ab^3-a^3b}Q^3 - \frac{2ae+3dc}{ab^3-a^3b}Q^2. \tag{5.2}$$

The Jacobian determinant of system Eq (5.1) can be stated in the next form

$$J(Q, Y) = \begin{vmatrix} 0 & 1 \\ \frac{4ae+6dc}{ab^3-a^3b} - \frac{12ab}{ab^3-a^3b}Q & 0 \end{vmatrix} = -\frac{4ae+6dc}{ab^3-a^3b} + \frac{12ab}{ab^3-a^3b}Q. \tag{5.3}$$

The equilibrium position (Q, Y) is center for $J(Q, Y) > 0$ and saddles for $J(Q, Y) < 0$, based on the bifurcation hypothesis for planar dynamics. Here, system Eq (5.1) contains two equilibrium points: $Q_1 = (0, 0)$ and $Q_2 = \left(\frac{\mathbf{2ae+3dc}}{\mathbf{3ab}}, 0\right)$ with $ab \neq 0$.

For $\omega_1\omega_2 > 0$:

(i) The Jacobian determinant, $J(Q_1) < 0$ and $J(Q_2) > 0$, is true for $\omega_1 > 0$ and $\omega_2 > 0$. Consequently, we can identify the equilibrium point Q_1 is an unstable saddle and the equilibrium position Q_2 is a stable center as shown in **Fig. 5**.

(ii) The Jacobian determinant, $J(Q_1) > 0$ and $J(Q_2) < 0$, is true for $\omega_1 < 0$ and $\omega_2 < 0$. Consequently, we can identify the equilibrium point Q_1 is a stable center and the equilibrium position Q_2 is an unstable saddle as shown in **Fig. 6**.

For $\omega_1\omega_2 < 0$:

(i) The Jacobian determinant, $J(Q_1) < 0$ and $J(Q_2) > 0$, is true for $\omega_1 > 0$ and $\omega_2 < 0$. Consequently, we can identify the equilibrium point Q_1 as an unstable saddle and the equilibrium position Q_2 as a stable center as shown in **Fig. 7**.

(ii) The Jacobian determinant, $J(Q_1) > 0$ and $J(Q_2) < 0$, is true for $\omega_1 < 0$ and $\omega_2 > 0$. Consequently, we can identify the equilibrium point Q_1 as a stable center and the equilibrium position Q_2 as an unstable saddle that corresponds to **Fig. 8**.

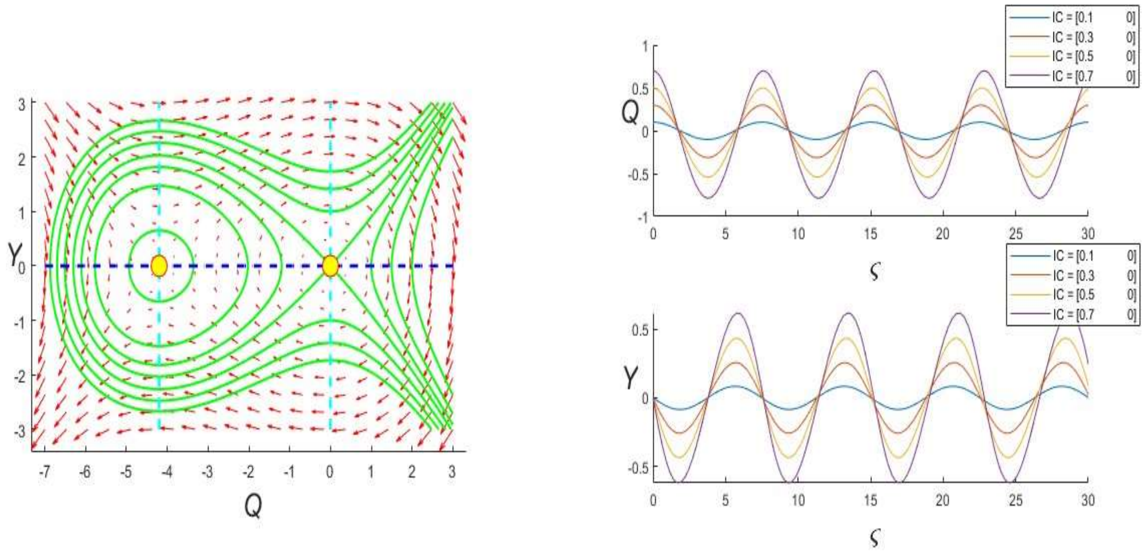

(a) (b)

Fig-5: Outlook of Eq (5.1) for $a = 10, b = 8, c = 20, d = -30, e = 39.6$. (a) Phase portrait, and (b) analogous outcome for wave variable ς.

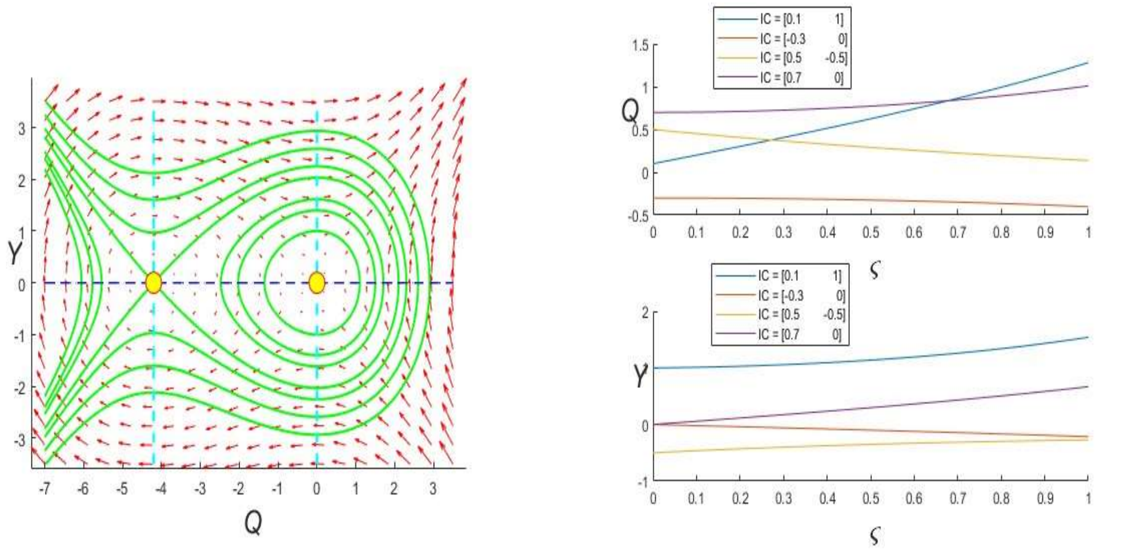

(a) (b)

Fig-6: Outlook of Eq (5.1) for $a = 8, b = 10, c = 20, d = -30, e = 49.5$. (a) Phase portrait, and (b) analogous outcome for wave variable ς.

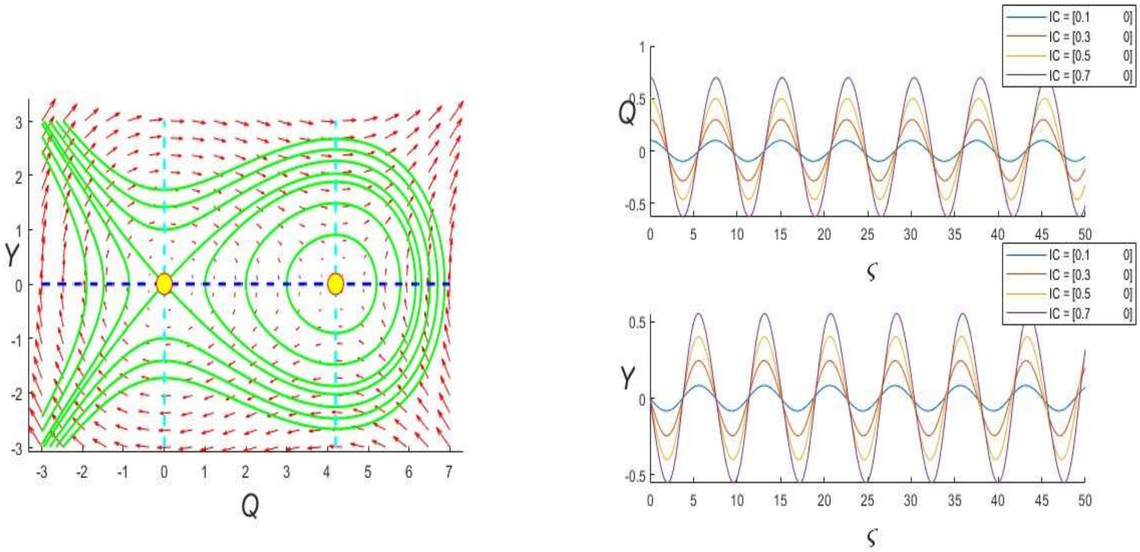

(a) (b)

Fig-7: Outlook of Eq (5.1) for $a = 8, b = 10, c = 20, d = 30, e = -49.5$. (a) Phase portrait, and (b) analogous outcome for wave variable ς.

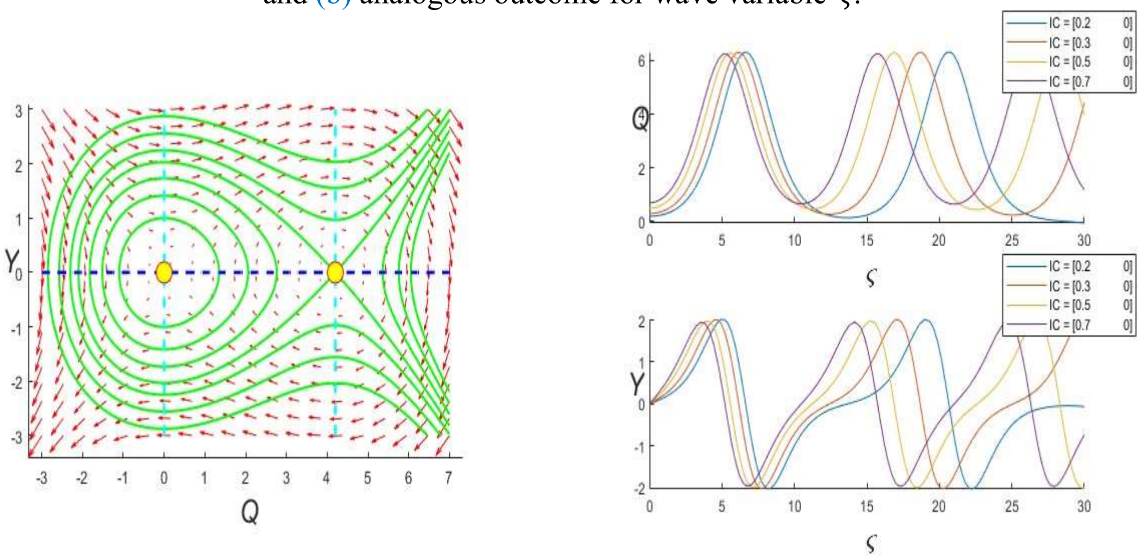

(a) (b)

Fig-8: Outlook of Eq (5.1) for $a = 10, b = 8, c = 20, d = 30, e = 39.6$. (a) Phase portrait, and (b) analogous outcome for wave variable ς.

6 Chaotic analysis with diverse chaos-detecting tools

The chaotic investigation of the underlying model is discussed in this segment using diverse chaos-detecting tools [26]. The arrangement of variables in Eq.(5.1) can be expressed as the next dynamical system to facilitate this examination.

$$\frac{\mathrm{d}Q}{\mathrm{d}\varsigma} = Y, \frac{\mathrm{d}Y}{\mathrm{d}\varsigma} = \omega_1 Q + \omega_2 Q^2 + \rho\cos(\gamma\varsigma), \tag{6.1}$$

for $\omega_1 = \frac{4ae+6dc}{ab^3-a^3b}$ and $\omega_2 = -\frac{6ab}{ab^3-a^3b}$ where the additional term $\rho\cos(\gamma\varsigma)$ indicates the disturbed term with intensity ρ and frequency γ. To reach our destination, diverse chaos-detecting tools like the bifurcation diagram, Lyapunov exponent plot, return map plot, power spectrum plot, 3D strange attractor diagram, and recurrence diagram of Eq.(5.1) are included in **Figs. 9-14**. We plot bifurcation diagrams in **Fig. 9** for $a = 2,\ b = 1,\ c = -0.3,\ d = 1/3,\ e = -0.45,\ \gamma = 4$ with primary value $(0,\ 0)$. In **Fig. 9a** and **9b**, the bifurcation patterns for parameters ω_1 and ω_2 show the discrete and dense pattern confirming the system's chaotic state. In **9c**, the bifurcation pattern for the parameter ρ, show how the system's environment is changing from stable to chaotic. We consider the parameter combinations $a = 83/14,\ b = 85/14,\ c = 1,\ d = 0.1,\ e = -5.23,\ \rho = 2.45,\ \gamma = 4.9$ with primary value $(0.2, 0.2)$ for the Lyapunov exponent diagram, the return map plot, and the power spectrum plot. We plot the Lyapunov exponent diagram in **Fig. 10**. The positive Lyapunov exponent confirms the presence of a chaotic state of the governing model. We also provide an iterative technique for calculating it numerically in **Table 1**. We plot the return map diagram in **Fig. 11**. The dense and scattered patterns in **Fig. 11a** and **Fig. 11b** show that the governing model is chaotic. We plot the power spectrum diagram in **Fig. 12**. There are many peaks in **Fig. 12a** and **Fig. 12b**'s broad frequency responses, which shows that the governing model is in a chaotic state. We plot the strange attractor diagram in **Fig. 13**. The irregular intricate patterns in **Fig. 13a** and **Fig. 13b** show that the governing model is in a chaotic state. We plot the recurrence plot in **Fig. 14**. The unpredictable behavior of **Fig. 14a** and **Fig. 14b** show that the governing model is in a chaotic state.

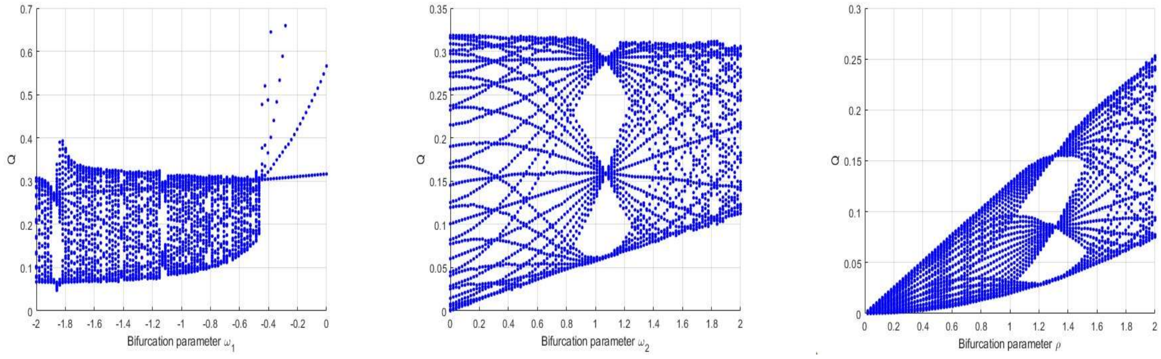

(a) (b) (c)

Fig-9: Bifurcation plot of Eq (6.1).

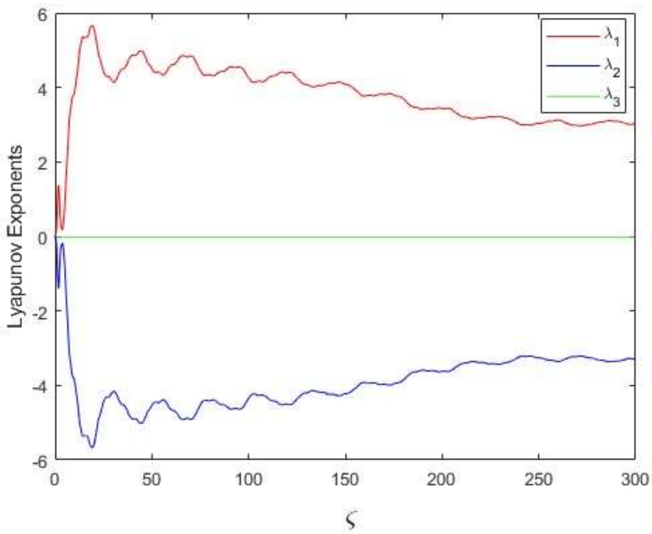

Fig-10: Lyapunov exponent plot of Eq (6.1).

Table 1: Successive iterations for Lyapunov exponents

Time	λ_1	λ_2	λ_3
30	4.1511	-4.1699	0.0000
60	4.5992	-4.6546	0.0000
90	4.5374	-4.6214	0.0000
120	4.3895	-4.501	0.0000
150	4.0806	-4.2197	0.0000
180	3.6862	-3.8528	0.0000
210	3.2263	-3.4193	0.0000
240	3.012	-3.23	0.0000
270	2.9801	-3.2231	0.0000
300	3.0336	-3.3032	0.0000

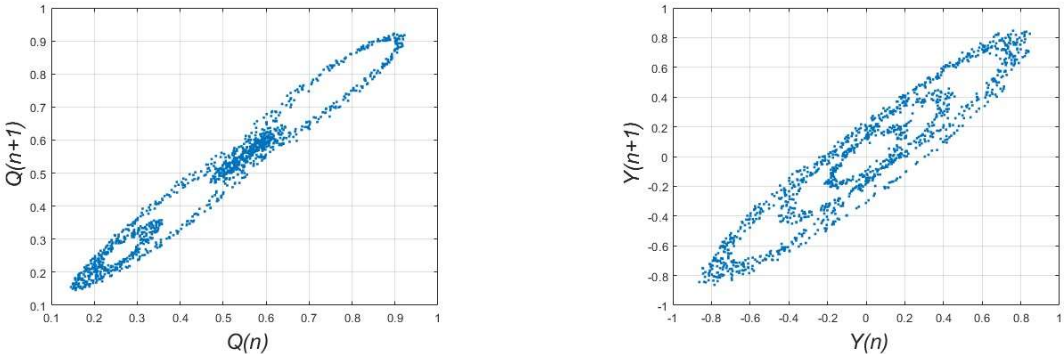

(a) For state variable Q (b) For state variable Y

Fig-11: Return map plot of Eq (6.1).

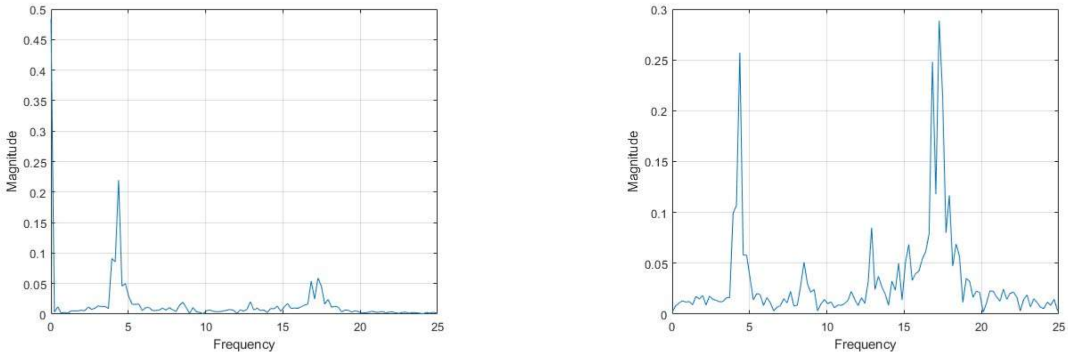

(a) For state variable Q (b) For state variable Y

Fig-12: Power spectrum plot of Eq (6.1).

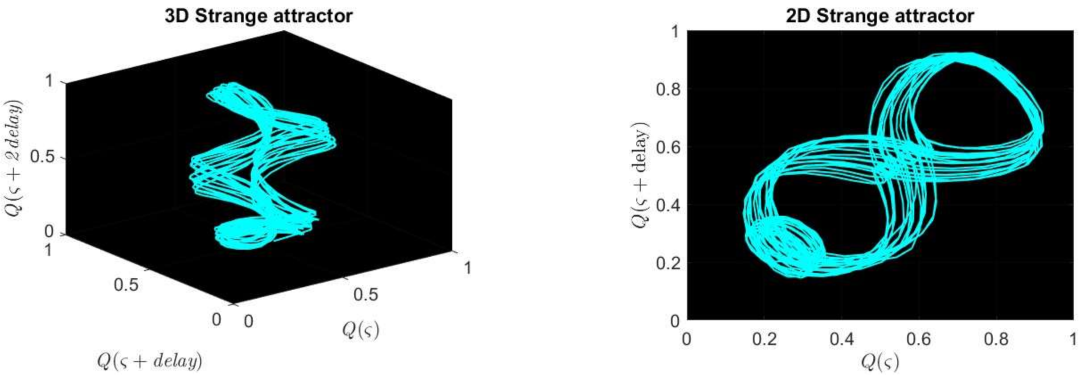

(a) (b)

Fig-13: Strange attractor of Eq (6.1).

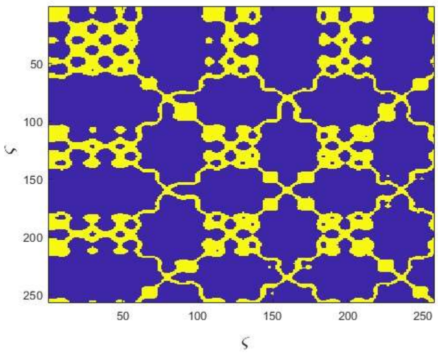

(a) For state variable Q

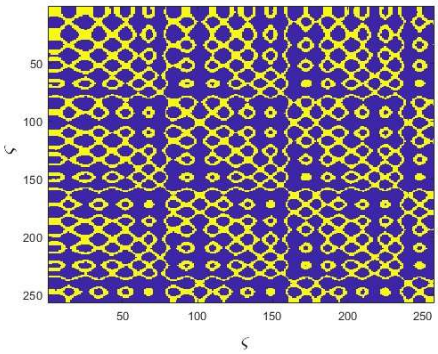

(b) For state variable Y

Fig-14: Recurrence plot of Eq (6.1).

7 Result's Novelty

section highlights the achievement and uniqueness of our results. By comparing the results of our study with previous research, including works by [27-30], we were able to accomplish our goal. Some reliable and efficient integration techniques have been used for the chosen model to describe soliton solutions. Rabie et al. got bright, dark, singular, and mixed dark-singular soliton results for this model [27] using the modified extended mapping method. Alsharidi and Junjua used the unified and modified extended tanh-expansion methods to make dark, bright, kink, and singular optical solitons [28] for this model in the form of a truncated M-fractional derivative. El-Ganaini and Al-Amr have developed this model, which yields a variety of exact results. They use the Jacobi elliptic expansion and the generalized Kudryashov procedures [29]. Tan and his co-authors used the parameter limit procedure [30] to come up with homoclinic and rogue wave solutions for the model mentioned above. Our findings differ from [27-30], but if we provide alternative values for certain settings, some results may be similar. Thus, our work is innovative in a few key areas, which we summarize as follows:

- We introduce and use the φ^6-model expansion method for this higher-dimensional nonlinear model, which has never been applied previously.

- Applying solutions that contain Jacobi, trigonometric, and hyperbolic forms, we discover novel dynamical optical solitons. This develops the solution opportunities of the selected model.
- This is the first research to examine the chaotic nature of the governing model using strange attractors, Lyapunov exponents, bifurcation diagrams, and other approaches.
- Since our employed technique works well and is flexible enough to handle diverse nonlinear evolution situations, it is helpful for further study.

8 Conclusion

We successfully applied the φ^6-model expansion method to the DSKP structure in (4+1) dimensions. This study makes the model more useful for plasma physics, wave science, coastal engineering, and fluid mechanics by adding new optical soliton solutions and dynamic information. Using Jacobi elliptic, hyperbolic, and trigonometric forms, our expansion technique gives us more possible solutions than other methods. Additionally, the planar dynamic assessment expands our understanding of stability, bifurcation, chaos, and other issues that previous studies have not fully explored. We also use different chaos-identification methods, such as Lyapunov exponents, bifurcation plots, strange attractors, and others, to identify how chaotic the governing model is. This comprehensive approach broadens the scope of soliton theory and provides a robust framework for future research in these interconnected fields. Our findings pave the way for innovative applications and deeper insights into wave dynamics and fluid behavior by addressing previously overlooked complexities.

Authors' contributions: Mohammad Safi Ullah: Writing-original draft, Software, Methodology; **M. Zulfikar Ali**: Writing-review and editing, Supervision, Validation; **Harun-Or Roshid**: Supervision, Validation.

Conflict of interest: The authors declare no conflict of interest.

Funding: Not applicable.

Data availability statement: All data generated or analysed during this study are included in this article.

References

[1] Ma, W.X.: Sasa-Satsuma type matrix integrable hierarchies and their Riemann-Hilbert problems and soliton solutions. Physica D 446l 133672 (2023).

[2] Ullah, M.S., Ali, M.Z., Roshid, H.O.: Bifurcation analysis and new waveforms to the first fractional WBBM equation. Sci Rep 14 11907 (2024).

[3] Ullah, M.S., Ali, M.Z., Roshid, H.O.: Bifurcation analysis and new waveforms to the fractional KFG equation. Partial Differ. Equ. Appl. Math. 10 100716 (2024).

[4] Alam, N., Ma, W.X., Ullah, M.S., Seadawy, A.R., Akter, M.: Exploration of soliton structures in the Hirota–Maccari system with stability analysis. Mod Phys Lett B, 2450481 (2024).

[5] Ganie, A.H., Wazwaz, A.M., Seadawy, A.R., Ullah, M.S., Roshid, H.O., Afroz, H.D. Akter, R.: Application of three analytical approaches to the model of ion sound and Langmuir waves. Pramana - J Phys 98 46 (2024).

[6] Ma W.X., Lee J.H., A transformed rational function method and exact solutions to the 3+1 dimensional Jimbo-Miwa equation, Chaos Solitons Fract 42(3) 1356–1363 (2009).

[7] Ganie, A.H., AlBaidani, M.M., Wazwaz, A.M., Ma, W.X., Shamima, U., Ullah, M.S.: Soliton dynamics and chaotic analysis of the Biswas–Arshed model. Opt Quantum Electron. 56 (8), 1379 (2024).

[8] Javed, S., Ali, A., Ahmad, J., Hussain, R.: Study the dynamic behavior of bifurcation, chaos, time series analysis and soliton solutions to a Hirota model. Opt Quant Electron **55**, 1114 (2023).

[9] Akter, M., Ullah, M.S., Wazwaz, A.M., Seadawy, A.R.: Unveiling Hirota-Maccari model dynamics via diverse elegant methods. Opt Quant Electron 56 6714 (2024).

[10] Ullah, M.S., Ali, M.Z., Roshid, H.O.: Bifurcation, chaos, and stability analysis to the second fractional WBBM model. PloS One. 19 (7), e0307565 (2024).

[11] Seadawy, A.R., Bilal, M., Younis, M., Rizvi, S.T.R., Althobaiti, S., Makhlouf, M.M.: Analytical mathematical approaches for the double-chain model of DNA by a novel Computational technique. Chaos Solitons Fract. **144**, 110669 (2021).

[12] Ali, A., Ahmad, J., Javed, S., Rehman, S.U.: Exact soliton solutions and stability analysis to (3 + 1)-dimensional nonlinear Schrödinger model, Alex Eng J. **76**, 747-756 (2023).

[13] Ali, A., Ahmad, J., Javed, S.: Exploring the dynamic nature of soliton solutions to the fractional coupled nonlinear Schrödinger model with their sensitivity analysis. Opt Quant Electron **55**, 810 (2023).

[14] Ali, A., Ahmad, J., Javed, S., Alkarni, S., Shah, N.A.: Investigate the dynamic nature of soliton solutions and bifurcation analysis to a new generalized two-dimensional nonlinear wave equation with its stability, Results Phys. **53**, 106922 (2023).

[15] Zhou, Q., Yao, D., Chen, F.: Analytical study of optical solitons in media with Kerr and parabolic-law nonlinearities. J. Mod. Opt. **60** (19), 1652-1657 (2013).

[16] Rehman, S.U., Bilal, M., Ahmad, J.: New exact solitary wave solutions for the 3D-FWBBM model in arising shallow water waves by two analytical methods. Results Phys. 25 104230 (2021).

[17] Sajid, N., Akram, G.: Novel solutions of Biswas-Arshed equation by newly φ^6-model expansion method, Optik, 211, 164564 (2020).

[18] Tipu, G.H., Faridi, W.A., Rizk, D., Myrzakulova, Z., Myrzakulov, R., Akinyemi, L.: The Optical exact soliton solutions of Shynaray-IIA equation with φ^6-model expansion approach. Opt Quant Electron. 56, 226 (2024).

[19] Ullah, M.S., Seadawy, A.R., Ali, M.Z., Roshid, H.O.: Optical soliton solutions to the Fokas–Lenells model applying the φ^6-model expansion approach. Opt Quant Electron. 55, 495 (2023).

[20] El-Shorbagy, M.A., Akram, S., Rahman, M.U.: Propagation of solitary wave solutions to (4+1)-dimensional Davey–Stewartson–Kadomtsev–Petviashvili equation arise in mathematical physics and stability analysis, Part Diff Equ Appl Math, 10, 100669 (2024).

[21] Junjua, M.U.D., Mostafa, A.M., AlQahtani, N.F., Bekir, A.: Impact of truncated M-fractional derivative on the new types of exact solitons to the (4+1)-dimensional DSKP model. Mod Phys Lett B. 38(32), 2450313 (2024).

[22] Fokas, A.S.: Integrable nonlinear evolution partial differential equations in 4+ 2 and 3+ 1

dimensions. Phys Rev Lett. 96(19), 190201 (2006).

[23] Rehman, H.U., Said, G.S., Amer, A., Ashraf, H., Tharwat, M.M., Abdel-Aty, M., Elazab, N.S., Osman, M.S.: Unraveling the (4+1)-dimensional Davey-Stewartson-Kadomtsev Petviashvili equation: Exploring soliton solutions via multiple techniques. Alex Eng J. 90, 17–23 (2024).

[24] Talafha, A.M., Jhangeer, A., Kazmi, S.S.: Dynamical analysis of (4 +1)-dimensional Davey Srewartson Kadomtsev Petviashvili equation by employing Lie symmetry approach. Ain Shams Eng J. 14(11), 102537 (2023).

[25] N. Alam, M. S. Ullah, T. A. Nofal, H. M. Ahmed, K. K. Ahmed, and M. A. AL-Nahhas, Novel dynamics of the fractional KFG equation through the unified and unified solver schemes with stability and multistability analysis, Nonlin. Eng. 13(1), 20240034 (2024).

[26] Almheidat, M., Alqudah, M., Alderremy, A.A. et al. Lie-bäcklund symmetry, soliton solutions, chaotic structure and its characteristics of the extended (3 + 1) dimensional Kairat-II model. Nonlinear Dyn (2024). https://doi.org/10.1007/s11071-024-10325-3.

[27] Rabie, W.B., Khalil, T.A., Badra, N., Ahmed, H.M., Mirzazadeh, M., Hashemi, M.S.: Soliton Solutions and Other Solutions to the (4+1)-Dimensional Davey– Stewartson–Kadomtsev–Petviashvili equation using modified extended mapping method. Qual. Theory Dyn. Syst. 23, 87 (2024).

[28] Alsharidi, A.K., Junjua, M.U.D.: Kink, dark, bright, and singular optical solitons to the space–time nonlinear fractional (4+1)-dimensional Davey–Stewartson–Kadomtsev–Petviashvili model. Fractal Fract. 8, 388 (2024).

. [29] El-Ganaini, S., Al-Amr, M. O.: New abundant wave solutions of the conformable space–time fractional (4+1)-dimensional Fokas equation in water waves. Comput Math Appl. 78(6) 2094-2106 (2019).

[30] Tan, W., Dai, Z. D., Xie, J. L., Qiu, D. Q.: Parameter limit method and its application in the (4+1)-dimensional Fokas equation. Comput Math Appl. 75(12) 4214-4220 (2018).